Original Article

Construction of a lung cancer 3D culture model based on alginate/gelatin micro-beads for drug evaluation

Ziying Zhao[1,2#], Xiaoqing Feng[1,2#], Huijuan Wu[3], Shuisheng Chen[1], Changsong Ma[4], Ziyun Guan[5], Luwen Lei[6], Kejing Tang[1,7], Xiao Chen[1], Yong Dong[8], Yubo Tang[1]

[1]Department of Pharmacy, the First Affiliated Hospital of Sun Yat-sen University, Guangzhou, China; [2]School of Pharmaceutical Sciences, Sun Yat-sen University, Guangzhou, China; [3]Department of Medical Science Research, the Sixth Affiliated Hospital, School of Medicine, South China University of Technology, Foshan, China; [4]Department of Orthopaedics, the Second Affiliated Hospital of Guangzhou Medical University, Guangzhou, China; [5]Department of Emergency, the Sixth Affiliated Hospital, School of Medicine, South China University of Technology, Foshan, China; [6]Department of Pharmacy, the Sixth Affiliated Hospital, School of Medicine, South China University of Technology, Foshan, China; [7]Division of Pulmonary and Critical Care Medicine, the First Affiliated Hospital of Sun Yat-sen University, Guangzhou, China; [8]Division of Interventional Radiology, the First Dongguan Affiliated Hospital of Guangdong Medical University, Dongguan, China

Contributions: (I) Conception and design: Z Zhao, X Feng, Y Tang; (II) Administrative support: Y Tang; (III) Provision of study materials or patients: Z Zhao, S Chen, Y Tang; (IV) Collection and assembly of data: Z Zhao, X Feng, H Wu; (V) Data analysis and interpretation: Z Zhao, X Feng; (VI) Manuscript writing: All authors; (VII) Final approval of manuscript: All authors.

[#]These authors contributed equally to this work.

Correspondence to: Yubo Tang, PhD. Department of Pharmacy, the First Affiliated Hospital of Sun Yat-sen University, No. 58 Zhongshan Er Road, Guangzhou 510080, China. Email: tangyb6@mail.sysu.edu.cn; Yong Dong, PhD. Division of Interventional Radiology, the First Dongguan Affiliated Hospital of Guangdong Medical University, No. 42 Jiaoping Road, Dongguan 523710, China. Email: dy1234560319@163.com.

Background: Lung cancer is one of the most common malignant tumors worldwide. Despite advances in lung cancer treatment, patients still face challenges related to drug resistance and recurrence. Current methods for evaluating anti-cancer drug activity are insufficient, as they rely on two-dimensional (2D) cell culture and animal models. Therefore, the development of an *in vitro* drug evaluation model capable of predicting individual sensitivity to anti-cancer drugs would greatly enhance the success rate of drug treatments for lung cancer patients. The purpose of this research is to utilise conditional reprogramming technology to cultivate patient-derived lung cancer cells and to construct an *in vitro* 3D culture model using sodium alginate (SA) and gelatin. The aim is to study the biological characteristics of cells in the 3D culture model and to further investigate the sensitivity of anti-cancer drugs based on the alginate-gelatin 3D culture model. This approach provides new means and insights for personalized precision anti-cancer therapy and the development of new anti-cancer drugs.

Methods: Conditional reprogramming technology was used to generate conditionally reprogrammed lung adenocarcinoma cells (CRLCs). Alginate-gelatin hydrogel micro-beads were created to explore their potential use in the assessment of anti-cancer drugs. Cell proliferation was also examined using the MTS assay method. Live/dead staining was performed to estimate cell distribution and viability using calcein acetoxymethyl ester/propidium iodide (calcein-AM/PI) double staining. Protein expression was assessed by Western blot.

Results: The cells grown in the three-dimensional (3D) culture were in a state of continuous proliferation, and there was an obvious phenomenon of cell mass growth. The drug sensitivity assay results demonstrated that compared with the 2D-grown cells, the CRLCs grown in the alginate-gelatin hydrogel micro-beads exhibited more resistance to anti-cancer drugs. The results also showed that the 3D-cultured CRLCs showed greater protein expression levels of stem cell hallmarks, such as Nanog Homeobox (NANOG), SRY-Box Transcription Factor 2 (SOX-2), and aldehyde dehydrogenase 1 family member A1 (ALDH1A1), than the 2D-grown cells.

Conclusions: These findings suggest that the 3D hydrogel cell culture models more closely mimicked

the *in vivo* biological and clinical behavior of cells, and demonstrated higher innate resistance to anti-cancer drugs than the 2D cell culture models, and thus could serve as valuable tools for diagnosis, drug screening, and personalized medicine.

Keywords: 3D cell model; drug evaluation; cell culture

Submitted Jun 06, 2024. Accepted for publication Sep 25, 2024. Published online Oct 28, 2024.
doi: 10.21037/tlcr-24-490
View this article at: https://dx.doi.org/10.21037/tlcr-24-490

Introduction

According to statistics, lung cancer is the leading cause of cancer-related death in men, and the second highest cause of cancer-related death in women, second only to breast cancer (1,2). There are two main forms of lung cancer: non-small-cell lung cancer (which accounts for 85% of all lung cancer cases), including adenocarcinoma, squamous cell carcinoma and large cell carcinoma, and small-cell lung cancer (which accounts for 15% of all lung cancer cases) (3).

Antineoplastic agents have distinct individual differences in terms of drug sensitivity, which causes interindividual variation in therapeutic effects. Increases in drug resistance continue to be the growing threat to achieving cures in patients with cancer (4). Therefore, personalized drug evaluation platforms for patients need to be established to enable personalized treatment decisions.

Conditionally reprogrammed (CR) technology allows for the rapid and efficient expansion of primary tumor cells from humans in large quantities in a short period without the introduction of any exogenous genes (5,6). This technique is straightforward and highly efficient, and the cultured CR cells maintain their original genetic characteristics, making them a valuable research model for studying diseases and individualized drug sensitivity testing (7,8). In our previous work, it was demonstrated through short tandem repeats testing and second-generation sequencing analysis that CR tumor cells can maintain their original genetic characteristics (9).

Different drug evaluation models have their limitations. The two-dimensional (2D) monolayer cell culture model differs greatly from the real physiological conditions *in vivo* because cells are unable to maintain their complete morphology, tumor microenvironment (TME), and cell-extracellular matrix (ECM) interaction, resulting in discrepancies in cell differentiation, proliferation, and cellular functions (10,11). Patient-derived xenograft models can better represent the TME *in vivo*. However, constructing patient-derived xenograft models is complex, time-consuming, and costly. Despite the significant anatomical and physiological similarities between animals and humans, which make them suitable models for research, genetic differences and ethical constraints limit their clinical application. Additionally, studying the relationship between drug resistance and microenvironmental regulation in xenograft models is relatively challenging (11,12). However, the use of three-dimensional (3D) cell culture models has been shown to be an efficient way to maintain the cell morphology and the cell–cell interaction (13). 3D cell culture models provide more relevant tumor models that resemble real physiological conditions and can be used to build personalized drug screening platforms (14). The

Highlight box

Key findings

- This work provides valuable tools for lung cancer diagnosis, drug screening, and treatment.

What is known, and what is new?

- Three-dimensional (3D) cell culture models can be used to establish more relevant tumor models that resemble real physiological conditions and to build personalized drug screening platforms.
- Compared to two-dimensional cell culture models, 3D models show higher functional expression and higher anti-cancer drug resistance.

What is the implication, and what should change now?

- Used in the 3D cell culture model, sodium alginate (SA)-gelatin micro-beads exhibited heterogeneity and individual characteristics. Thus, SA-gelatin micro-beads could feasibly be used as a drug evaluation model to guide clinical medication decisions for patients. In the future, SA-gelatin micro-beads could be used for personalized drug screening to improve the accuracy and efficiency of clinical drug use.

construction of organoids suffers from low success rates, lengthy procedures, high costs, and the inability for long-term cultivation. In contrast, 3D cell models allow for the rapid acquisition of a large number of primary human cells within a short period, without altering the cells' inherent genetic characteristics, making them more advantageous as an *in vitro* drug screening model.

3D models are widely used in medical research because of their unique advantages (15). 3D models can combine the experimental advantages of *in vitro* research (e.g., long-term expansion, freezing preservation, and a low cost) with the advantages of *in vivo* research (e.g., providing cells with more realistic physiological conditions) (16). Currently, 3D models have been successfully used in several types of cancer, including malignant melanoma (17), colorectal cancer (CRC) (18), prostate cancer (19), ovarian cancer (20), breast cancer (21), and lung cancer (22). To date, 3D cell culture models have been widely used in studies, such as drug discovery, disease modelling, and drug screening studies (23). Notably, the pathophysiology of breast cancer has been studied through the construction of 3D culture models (24). Sun *et al.* established 3D cell culture models of CRC and colorectal liver metastasis, and found a strong correlation between drug responses in the 3D cell culture model and clinical effects (25).

Hydrogels, which are common materials for cell encapsulation, can be used to develop 3D models that are structurally similar to the cell-ECM interaction. SA is one of the most broadly studied and applied hydrogels. Alginate is a naturally occurring anionic polymer and has been widely used in many biomedical applications and tumor research studies because of its good biocompatibility and biodegradability (26,27). However, alginate cannot provide sufficient biological cues for cells to attach (28). Gelatin is made of hydrolysate from collagen, which is the main component of the ECM and retains arginyl-glycyl-aspartic acid peptide that can improve cell adhesion and proliferation (29,30). The addition of gelatin can improve the biocompatibility of SA microspheres (31).

In this study, we constructed a 3D cell-laden system with similar mechanical and biological properties to tissues, and we simulated the *in vivo* environment of lung cancer by mixing cancer cells with alginate and gelatin for the anti-cancer drug evaluation. In this study, we successfully constructed 3D culture models of lung cancer cells derived from nine patients. The physical properties of the 3D beads and the cytocompatibility of the alginate and gelatin were examined. We demonstrated that the expression levels of stemness proteins were higher in the 3D micro-beads than the 2D monolayer beads. Finally, the sensitivities of the anti-cancer drugs in the 3D models and the 2D monolayer models were compared. We hope that this method can be further applied in the 3D cell-laden system field and our findings can provide insights into the field of personalized and precision therapy. We present this article in accordance with the MDAR reporting checklist (available at https://tlcr.amegroups.com/article/view/10.21037/tlcr-24-490/rc).

Methods

Materials

Alginate, gelatin, high-glucose Dulbecco's modified eagle medium (DMEM), and fetal bovine serum were purchased from Thermo Fisher Scientific, USA. Calcium chloride was obtained from Shanghai Aladdin Biochemical Technology Co., Ltd., China. Collagenase IV was purchased from MP Biomedicals, USA. The cell proliferation MTS assay kit was obtained from Promega, USA. The calcein-AM/PI double-staining kit, Radio Immunoprecipitation Assay Lysis buffer (RIPA), and phenylmethylsulfonyl fluoride (PMSF) were purchased from Beyotime Biotech Inc., Shanghai, China. Rho kinase (ROCK) inhibitor Y27632, carboplatin, cisplatin, paclitaxel, docetaxel, vinorelbine, gemcitabine, osimertinib, and gefitinib were purchased from MedChemExpress, USA. The primary antibodies were against glyceraldehyde-3-phosphate dehydrogenase (GAPDH), NANOG, ALDH1A1, and SOX-2. GAPDH (CAT: 2118) was purchased from Cell Signaling Technology, USA. NANOG (CAT: 14295-1-AP), ALDH1A1 (CAT: 15910-1-AP), and SOX-2 (CAT: 11064-1-AP) were purchased from the Proteintech Group, USA. The goat anti-mouse antibody (CAT:7076) and goat anti-rabbit antibody (CAT:7074) were purchased from Cell Signaling Technology, USA. A 5× loading buffer (BioRad, USA) was added to the protein samples in 1:4 dilution and mixed. The PC-9 cells were purchased from Meisen Chinese Tissue Culture Collections (Meisen CTCC, China, CTCC-003-0204). The Swiss-3T3-J2 cells were purchased from American Type Culture Collection (ATCC, USA, CRL-1658).

Preparation of alginate-gelatin hydrogel precursor

The SA solution at a concentration of 4% (w/v, autoclaved) and gelatin aqueous solution at concentrations of 0.5% and 1% (w/v), sterilized by a 0.22-μm filtration membrane (Merck

Table 1 List of lung cancer samples used to establish patient-derived micro-beads

Case	Gender	Age (years)	Lung cancer type	Type of gene mutation
Patient-1	Male	40	Adenocarcinoma	NA
Patient-2	Female	67	Adenocarcinoma	EGFR L858R
Patient-3	Female	68	Adenocarcinoma	NA
Patient-4	Female	59	Adenocarcinoma	EGFR L858R, T790M
Patient-5	Male	56	Adenocarcinoma	NA
Patient-6	Male	66	Adenocarcinoma	NA
Patient-7	Male	81	Adenocarcinoma	NA
Patient-8	Female	67	Adenocarcinoma	NA
Patient-9	Male	52	Adenocarcinoma	EGFR Del 19

NA, not applicable.

Millipore, Germany), were dissolved in ultrapure water. They were stored in a refrigerator (at 4 ℃) for later use.

Patient-derived lung tumors

Fresh lung tumor tissues were collected from patients who underwent surgical resection at the First Affiliated Hospital, Sun Yat-sen University (Guangzhou, China). The study was conducted in accordance with the Declaration of Helsinki (as revised in 2013). The study was approved by the Ethics Committee of the First Affiliated Hospital, Sun Yat-sen University (No. [2018]-153) and informed consent was taken from all the patients. The surgically removed samples were stored in a sterile centrifugal tube for further operation. The patients' information is set out in *Table 1*.

Digestion of patient-derived lung tumor tissues

The patient-derived tumor tissues were removed from the preservation solution and quickly immersed in 95% ethanol for disinfection (less than 3 seconds) and then washed three times with phosphate buffer solution (PBS), split into 2–3 mm pieces, and centrifuged at 300 g for 5 minutes. Each sample was then digested in a reagent supplemented with advanced Dulbecco's modified eagle medium/Nutrient Mixture F-12 (DMEM/F12), containing 2.5 mg/mL of collagenase IV and 0.1 mg/mL of DNase I, and placed in a water bath at 37 ℃ for 6 hours. Subsequently, the solution was filtered through a 100-μm cell mesh sieve (Biologix Biotech Co., Ltd. , Shandong, China) followed by centrifugation at 500 g for 5 minutes and washed with PBS. This study utilized irradiated Swiss-3T3-J2 mouse fibroblast cells and Rho kinase (ROCK) inhibitor Y27632 for cell culture.

Cell culture

The SA solution (4%) and gelatin aqueous solution (0.5% or 1%) were mixed at ratios of 3:1 or 4:1 for later use. The cell pellet was resuspended using a sodium alginate (SA)-gelatin mixture, adjusting the cell density to 5×10^5/mL. Next, the alginate-gelatin hydrogel mixed with the cells was extruded through 1-mL syringes and slowly dropped into the calcium chloride ($CaCl_2$) solution (2%, autoclaved). The solution was then allowed to stand for 10 minutes to ensure adequate cross-linkage. After being washed with PBS three times, the 3D micro-beads were stored in high-glucose DMEM. The cells were collected by adding sodium citrate to dissolve the 3D micro-beads.

Scanning electron microscope analysis of cell micro-beads

After three days of culturing, some freeze-dried cell micro-beads were examined by scanning electron microscope (SEM) (Hitachi, Japan). To improve their conductivity, the completely freeze-dried cell micro-beads were sputter coated with gold on the surface and were scanned on a SU8100 SEM at voltage of 3.0 kV.

Cytocompatibility of the alginate-gelatin hydrogel

The PC-9 cells and CRLCs were centrifuged, and resuspended by alginate-gelatin hydrogel precursor to adjust

the cell density to 5×10^5 cells/mL as a cell-hydrogel mixture. The proliferation activity of the PC-9 cells and CRLCs was assayed by MTS on days 1, 3, 5, and 7. Each cell micro-bead was placed with 10 µL of MTS solution and 90 µL of fresh medium in 96-well plates. After incubation for 4 hours, the absorbance of the solution at 490 nm was measured by a microplate reader (Thermo Fisher Scientific, USA). For 2D culture, 3,000 cells were seeded in 96-well plates. After incubating until the time of testing, medium in each well was replaced with 10 µL of MTS solution and 90 µL of fresh medium. Similarly, the OD values were detected after incubating at 37 ℃ for 2 h. The cell viability rate was the ratio of the OD value of the experimental group to the OD value of the control group.

Live/dead staining

Live/dead staining was performed to estimate the cell distribution and viability using a calcein-AM/PI double-staining kit. After incubation for 2 hours, the live/dead cell staining of the micro-beads was imaged under confocal microscopy (Leica, Germany).

Drug screening

MTS was used to measure the effects of the drugs in the 2D monolayer and 3D cell micro-bead models. After 5 days of culturing, the 2D monolayer cells, which were seeded in 96-well plates, and the 3D cell micro-beads were tested with therapeutic compounds for 4 days at 37 ℃ with dimethyl sulfoxide (DMSO) or DMEM used as the control. The following chemotherapeutics and targeted drugs were tested: carboplatin, cisplatin, paclitaxel, docetaxel, vinorelbine, gemcitabine, osimertinib, and gefitinib.

Western blotting

Protein expression was analyzed by Western blotting. In brief, after being washed twice with PBS, the cells were lysed in RIPA buffer containing PMSF and protease inhibitors on ice for 30 minutes, shaken and centrifuged (12,000 rpm, 15 minutes, 4 ℃). The supernatants were diluted with 5× loading buffer and then boiled at 100 ℃ for 5 minutes. Load samples quickly at a protein concentration of 30 µg per well. The proteins were run on 10% gradient Sodium dodecyl sulfate - polyacrylamide gel electrophoresis (SDS-PAGE) for separation and then transferred onto polyvinylidene difluoride membranes by electro-blotting before being blocked with 5% bovine serum in Tris-buffered saline buffer containing 0.1% Tween 20 (TBST) for 60 minutes at room temperature. The membranes were washed with TBST three times for 10 minutes each time, and then incubated overnight at 4 ℃ with the following primary antibodies: GAPDH, NANOG, ALDH1A1, and SOX-2. After being washed three times with TBST, the membranes were incubated with secondary antibodies for 1 hour. Protein expression was next visualized using Enhanced chemiluminescence (ECL) reagents (Thermo Fisher Scientific, USA) on the ChemiDoc MP imaging system (BioRad, USA).

Statistical analysis

All the data are expressed as the mean ± standard deviation of at least three individual biological experiments. Comparisons between two groups were performed using Student's *t*-test, while comparisons among multiple groups were conducted using one-way analysis of variance (ANOVA). Significance levels were set at *, $P<0.05$, **, $P<0.005$, ***, $P<0.001$, ****, $P<0.0001$, and ns = not significant ($P>0.05$).

Results

The establishment and characterization of the cell micro-beads

In this study, alginate-gelatin hydrogel was used to fabricate the cell micro-beads. We mixed 4% alginate with 0.5% (w/v) or 1% (w/v) gelatin at the ratios of 3:1 or 4:1. After the cells were resuspended in the alginate-gelatin hydrogel, the crosslink between the 4% alginate and 2% $CaCl_2$ solution led to the completion of the cell micro-beads (*Figure 1A*). As the SEM images in *Figure 1B* show, the micro-bead was nearly a sphere in shape and had a porous structure, which enabled cell proliferation and adhesion. The average diameter value of the micro-beads from group 1 was 0.2728±0.00227 cm, and the micro-bead diameters showed a normal distribution (*Figure 1C*). Additionally, we performed particle size analysis on three different batches of alginate-gelatin microbeads. There was no difference in the diameters of the alginate beads in groups 1–3, which showed the consistency and stability of the cultivation approaches (*Figure 1D*).

Morphological changes of the cells in the micro-beads

The PC-9 cells were cultured in alginate-gelatin hydrogel

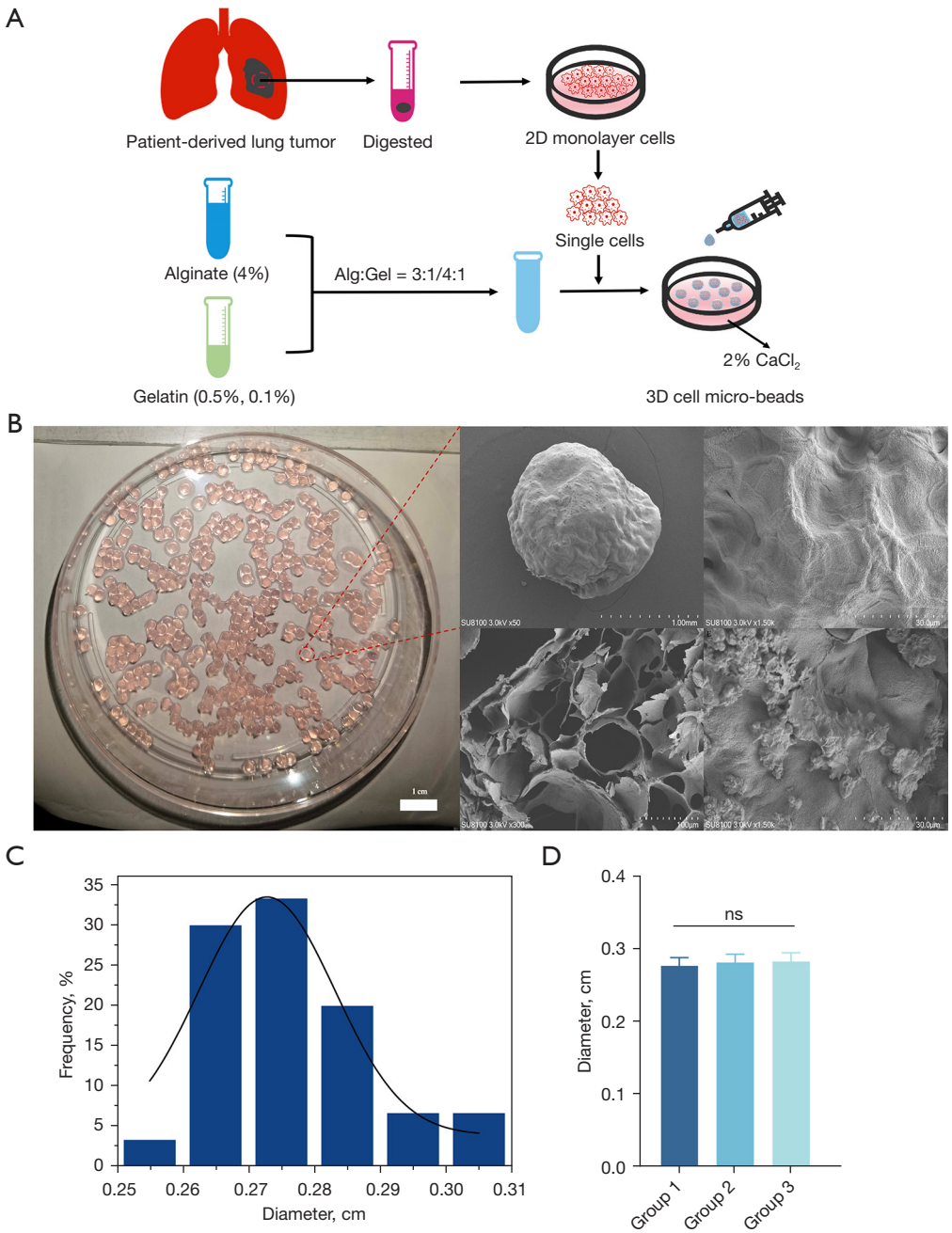

Figure 1 The establishment and characterization of the cell micro-beads. (A) Workflow of the alginate-gelatin hydrogel and cell micro-bead culture preparation. (B) SEM images of the cell micro-beads with the PC-9 cells. (C,D) The diameters of the micro-beads. The particle size of the microbeads was analyzed using the Image J software. The results of the particle size analysis were then processed with OriginPro 8.5 software, employing the Gauss function for nonlinear curve fitting. (C) The diameter of the micro-beads from group 1 showed a normal distribution. (D) Groups 1–3 are different batches of alginate-gelatin microbeads. The data are presented as mean ± SD (n=30). Alg, alginate; Gel, gelatin; ns, not significant; SEM, scanning electron microscope; SD, standard deviation.

in which the SA solution (4%) and gelatin aqueous solution (0.5% or 1%) were mixed at ratios of 3:1 or 4:1 (*Figure 2A*). We observed that similar multicellular structures, which looked like clusters of grapes, formed in different alginate-gelatin hydrogels after culturing for 3 days. Conversely, the cells derived from patients that were cultured in alginate-gelatin hydrogel for 7 days had multicellular structures that looked like spheres (*Figure 2B*,*2C*). The PC-9 cells and the cells derived from patients cultured in micro-beads for 7 days formed larger multicellular structures day by day (*Figure 2A*,*2C*). Cells were observed growing in alginate-gelatin microbeads with varying concentrations of alginate and gelatin. It was found that cells formed multicellular structures earlier in microbeads composed of 4% alginate and 1% gelatin in a 4:1 ratio. Considering the higher stiffness of tumor tissue, subsequent studies will use alginate-gelatin microbeads constructed with 4% alginate and 1% gelatin in a 4:1 ratio.

The viabilities of the cells in the 2D monolayer and 3D micro-bead models

The PC-9 cells and the cells derived from patients in micro-beads underwent live/dead staining. It was observed that both the PC-9 cells and the cells derived from patients were alive in the micro-beads (*Figure 3A*). We further cultured the PC-9 cells and the cells derived from patients in the 2D monolayer and 3D micro-beads for 7 days. The cell proliferation curve used the cell viability value on day 1 as the baseline viability value. Relative viability values at each time point were calculated in comparison to this baseline, and the proliferation curve was plotted accordingly. Cells cultured in SA-gelatin microspheres exhibited a flatter growth curve and a lower proliferation rate compared to cells cultured in 2D conditions (*Figure 3B-3D*). There was no significant difference in the cell viabilities of the different concentrations of alginate-gelatin hydrogel at day 7. Thus, cells can maintain good viability and continue to grow and proliferate within micro-beads of different compositions (*Figure 3D*). We further tested the viabilities of the cells derived from patients 1–3 in the micro-beads and found that the cells derived from patient 1 in the 3D micro-beads had higher proliferation rate than those derived from patients 2 and 3. Thus, there were differences in the cell proliferation of the cells derived from different patients (*Figure 3E*).

The expression levels of the stemness proteins were significantly higher in the 3D micro-bead model than the 2D monolayer model

The characteristics of the cancer stem cells (CSCs) play a pivotal role in tumor initiation, progression, and therapy resistance (32). The overexpression of the transcription factors, such as Sox2 and Nanog, contributes to the regulation of CSC phenotypes (33). We sought to examine whether the expression levels of the stemness proteins were significantly higher in the 3D micro-bead model than the 2D monolayer model. We found that compared with the 2D monolayer, the cells in the 3D micro-beads of both the PC-9 cells and the cells derived from patient 4 showed stronger expression levels of Nanog, SOX-2, and ALDH1A1 (*Figure 4*).

Personalized drug evaluation

The patient-specific sensitivities to anti-cancer drugs in the 3D bead culture and 2D monolayer culture were tested by MTS assays. After being cultured for 5–7 days, the cells in the 3D beads were treated with anti-cancer drugs for an additional 4 days (*Figure 5*). A list of the half maximal inhibitory concentration (IC_{50}) value of the anti-cancer drugs against the cells under the 2D and 3D culture conditions are shown in Table S1, which details the log IC_{50}. The results illustrated that the cells from different patients reacted differently to different drugs, and the 3D beads mostly had higher IC_{50} values than the 2D monolayer.

We found that the 3D models of different patients responded differently to different concentrations of different drugs. For example, the 3D models of patients 1, 6, and 7 were the most sensitive to gemcitabine, while the 3D models of patients 3, 5, and 8 were the most sensitive to cisplatin. The 3D models of different patients also showed different sensitivities to the same drug at the same concentration; for example, carboplatin was the least sensitive to the 3D models of most of the patients with the exception of patient 9.

Discussion

The survival benefits and cure rates for lung cancer patients have improved dramatically with the advent of molecular targeted therapy. Molecular targeted therapy has been widely used in the treatment of lung cancer, but there are

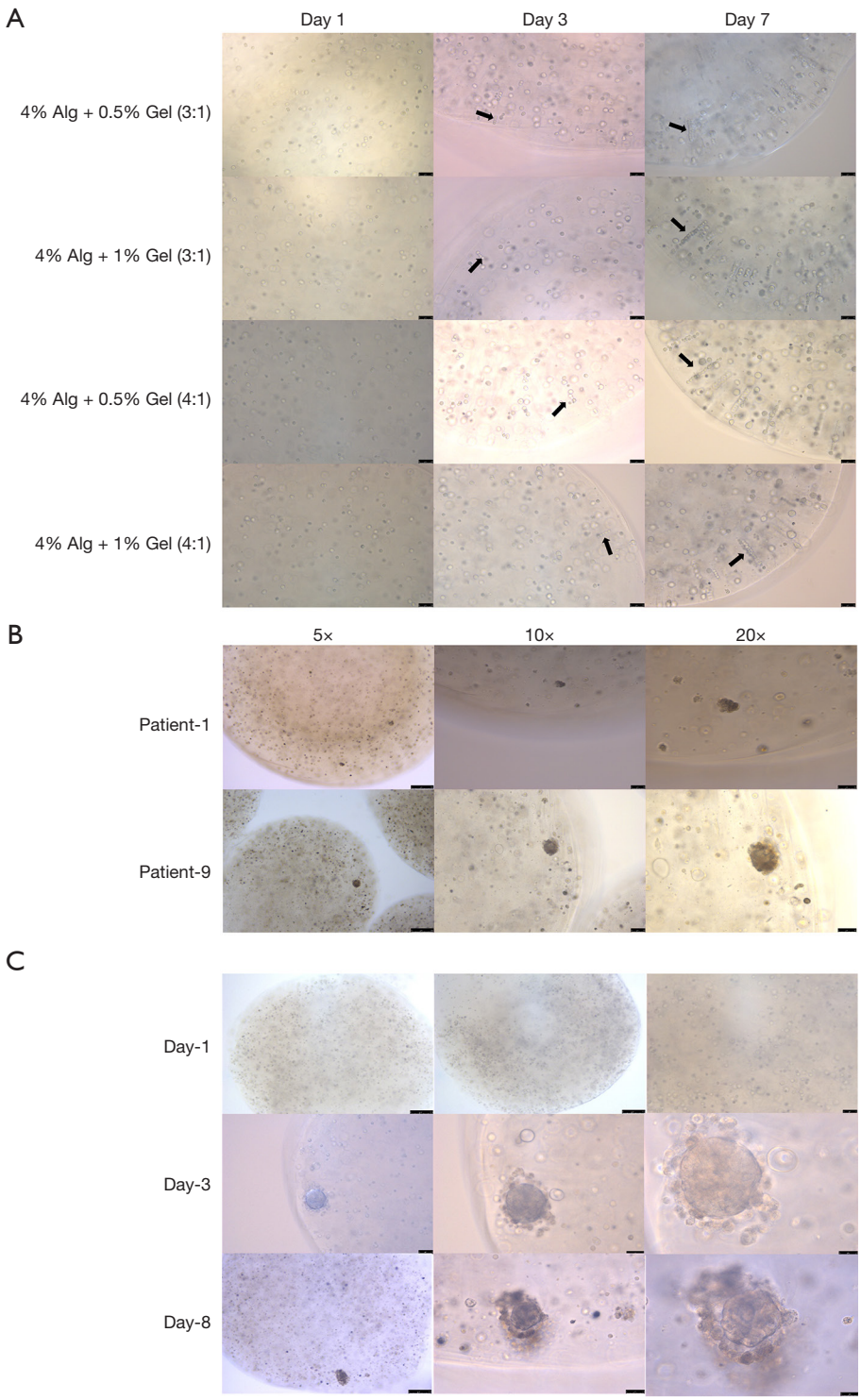

Figure 2 The morphological changes of the cells in the micro-beads. (A) PC-9 cells were cultured in the alginate-gelatin hydrogel in which the SA solution (4%) and gelatin aqueous solution (0.5% or 1%) were mixed at ratios of 3:1 or 4:1. Scale bars, 75 μm. The arrows indicate the multicellular structures. (B) The cells derived from patients 1, and 9 were cultured in alginate-gelatin hydrogel for 7 days; scale bars: 250 μm, 75 μm, 50 μm (from left to right). (C) The cells derived from patient 4 were cultured in alginate-gelatin hydrogel. Scale bars: day 1: 250 μm, 250 μm, 75 μm; day 3: 75 μm, 50 μm, 25 μm; day 8: 250 μm, 50 μm, 25 μm (from left to right). Alg, alginate; Gel, gelatin.

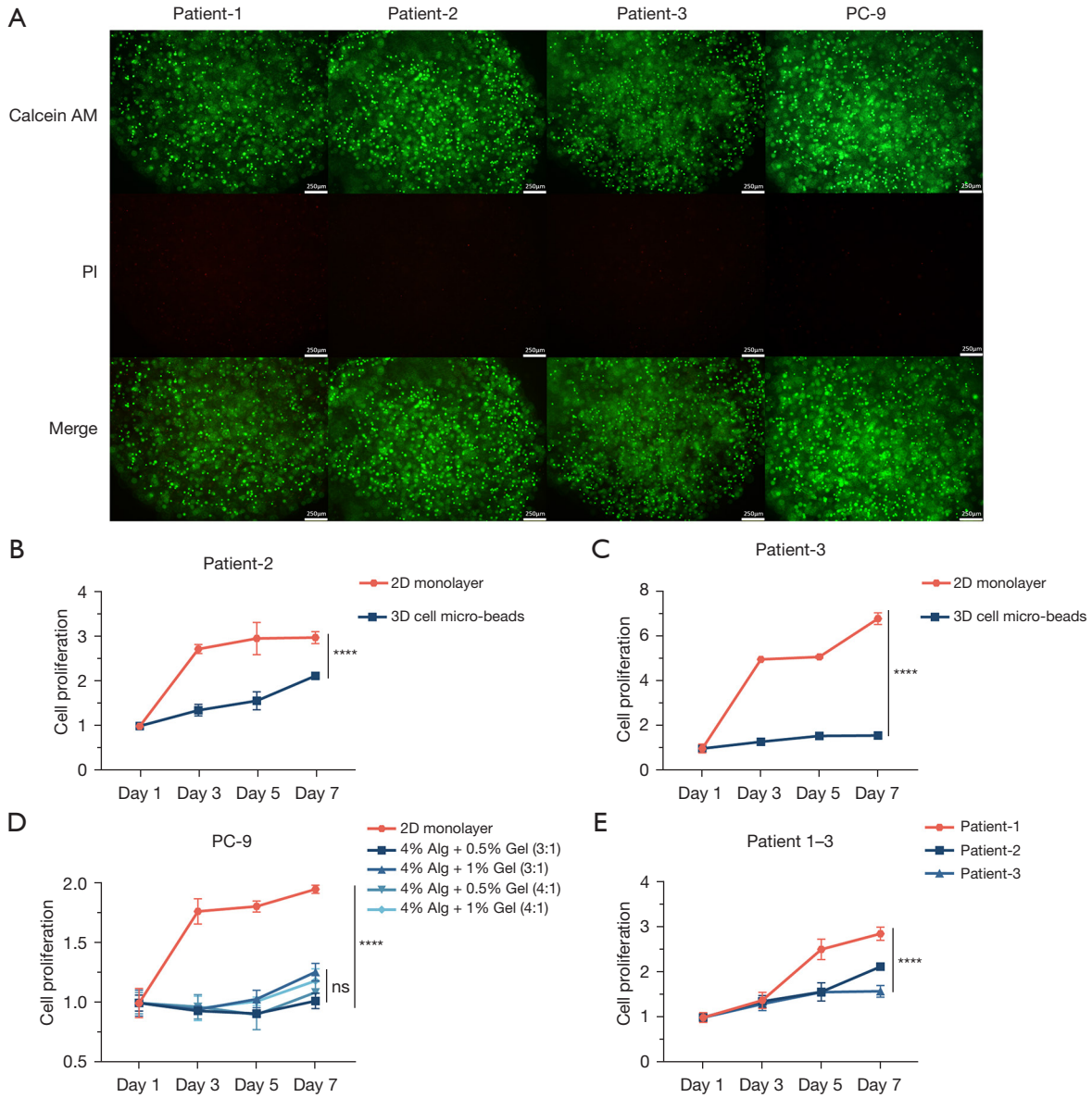

Figure 3 The cell viabilities of the cells in the 2D monolayer and 3D micro-bead models. (A) Live/dead staining (using a calcein-AM/PI double-staining kit) of cells of micro-beads at day 1 of culture. Scale bars, 250 μm. (B,C) Proliferation of cells derived from patients 2 and 3 in the 2D monolayer and 3D micro-bead models. (D) Proliferation of the PC-9 cells in the 2D monolayer and 3D micro-bead models. (E) Proliferation of cells derived from patients 1–3 in the 3D micro-bead models. ****, P<0.0001. The data are presented as mean ± SD (n=3). Calcein-AM, calcein acetoxymethyl ester; PI, propidium iodide; Alg, alginate; Gel, gelatin; 2D, two-dimensional; 3D, three-dimensional; SD, standard deviation.

still many problems with current lung cancer treatments. Molecular targeted therapy can only benefit a fraction of patients with specific tumor mutation genes. Additionally, due to epigenetic alterations, patients with the same genetic mutations still respond heterogeneously to the therapeutic effects (34,35). Therefore, the *in vitro* prediction of an individual's sensitivity to anti-cancer drugs would help improve the success rate of drug treatments.

Currently, there is no technology that can remodel various tumors *in vitro* with 100% accuracy. The 2D monolayer cell culture model is commonly used to evaluate the pharmaceutical activities of anti-cancer drugs because

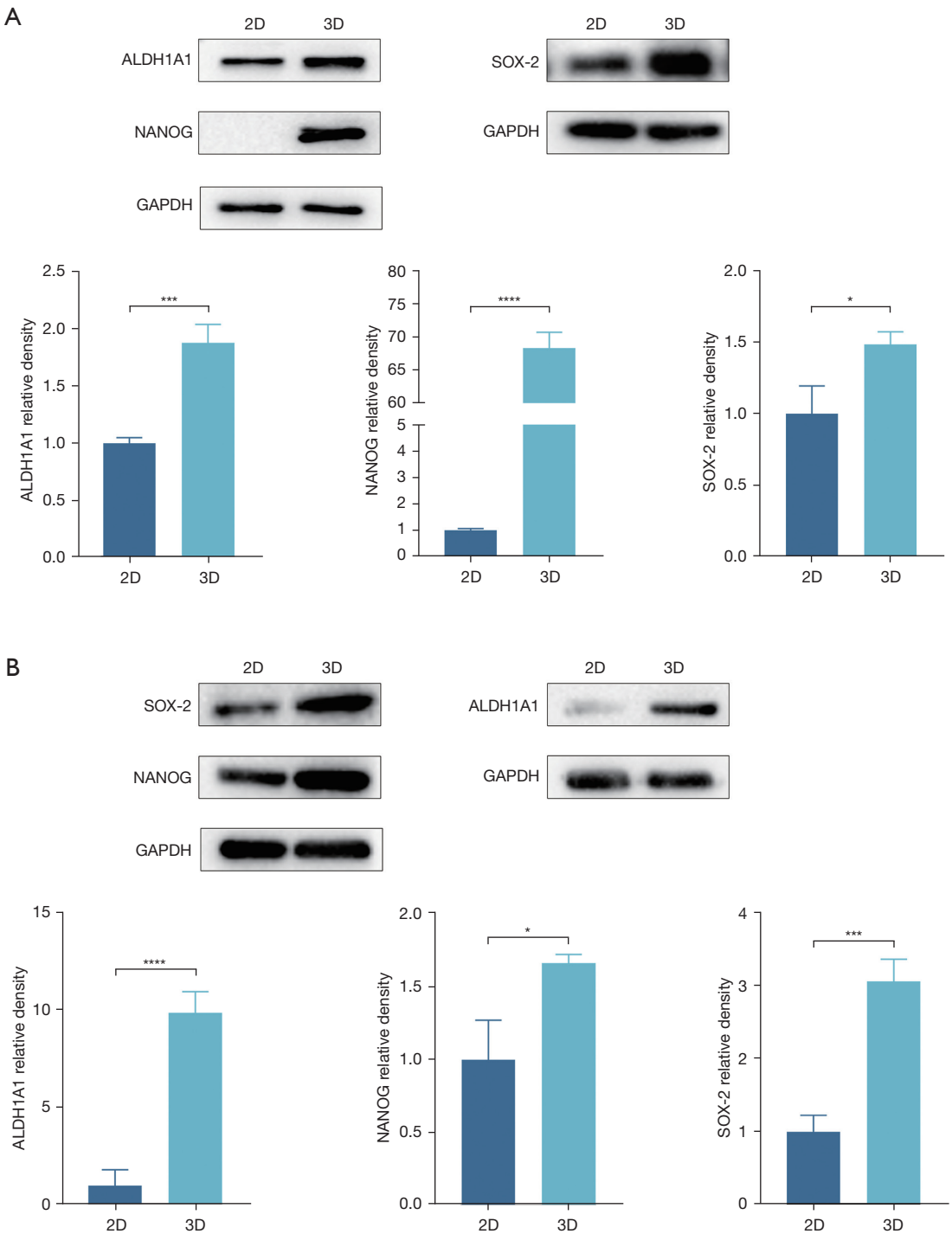

Figure 4 The expression levels of the stemness proteins. After being cultured in micro-beads for 7 days, protein expression testing was performed. (A) The expression levels of the stemness proteins of patient 4 were significantly higher in the 3D micro-bead model than the 2D monolayer model. (B) The expression levels of the stemness proteins of the PC-9 cells were significantly higher in the 3D micro-bead model than the 2D monolayer model. The data are presented as mean ± SD (n=3). *, P<0.05; ***, P<0.001; ****, P<0.0001. 2D, two-dimensional; 3D, three-dimensional; SD, standard deviation.

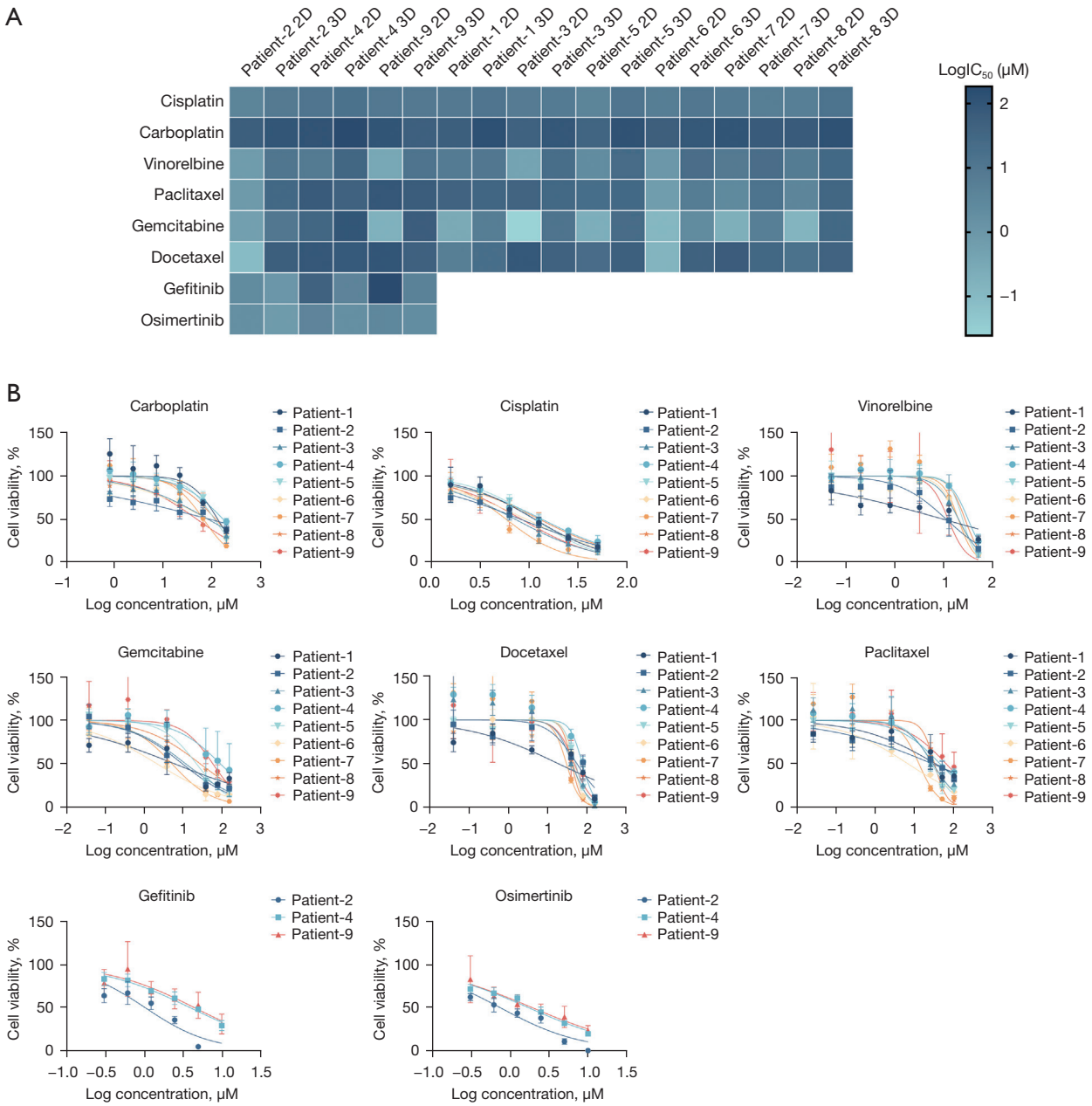

Figure 5 Drug evaluation of the cells under 2D and 3D culture conditions. (A) Heatmap of the logIC_{50} values for the anti-cancer drugs by applying nonlinear regression. (B) Dose-response curves for the anti-cancer drugs of the 3D models. The data are presented as mean ± SD (n=3). 2D, two-dimensional; 3D, three-dimensional; IC_{50}, half maximal inhibitory concentration; SD, standard deviation.

of its low cost and low technical threshold (36). However, the 2D monolayer cell culture model differs from the real physiological conditions of patients *in vivo*, which causes inaccurate drug responses and thus impedes the discovery of potential drug candidates (37).

In this study, we developed a 3D cell-laden system that aimed to establish lung cancer models that could more closely replicate either structures or functions *in vivo* for anti-cancer drug evaluations compared to 2D cultures. Currently, hydrogels can be processed by different methods that can represent human tumors, such as 3D bioprinting (38,39) and microfluidics (40). Our method is economical

and has a low technical threshold. Photo-initiator and UV light are often applied on gelatin meth-acryloyl solutions, which may cause oxidative stress and damage to DNA repair proteins; however, this issue did not arise in our method (41). In this study, we showed that cells can maintain good viability and continue to grow and proliferate within microbeads of different compositions. However, we did not investigate the effects of different concentration variations of $CaCl_2$. In other published works, we found that the increased concentration of calcium chloride and SA inhibits cell multiplication because of the excessive calcium ions and compact structure of the alginate capsules (42).

We found that alginate and gelatin do not restrict cell growth and proliferation. Cells in alginate-gelatin microbeads continue to proliferate and tend to form noticeable cell clusters. Compared to 2D culture conditions, 3D culture conditions enhance the spheroid formation ability of primary lung cancer cells and increase the expression of stemness proteins such as ALDH1A1, SOX2, and NANOG. This indicates that 3D cell culture can enhance the stemness of cells, making their characteristics more similar to those of *in vivo* tumor cells. We compared the sensitivities of anti-cancer drugs in traditional 2D cell culture models and 3D bead models, and found that the cells in the 3D bead models showed significantly higher resistance than those in the 2D models, which provides evidence of the higher resistance of the anti-cancer drugs of the cells in the 3D bead models than the 2D models. The results of targeted drug sensitivity testing showed that, compared to 2D culture conditions, cells cultured under 3D conditions exhibit higher sensitivity to targeted drugs. Similar to our study, Xiao *et al.* (43) constructed 3D models of non-small cell lung cancer cell lines HCC827, H1975, and PC-9 and found that the sensitivity of the EGFR-targeted drug cetuximab was significantly higher in the 3D models than in the 2D models. EGFR mutation-carrying cell lines displayed a more sensitive growth inhibition response to targeted drugs. Further comparison with *in vivo* drug sensitivity results in animal models indicated that the drug response results from the 3D tumor models had higher consistency with animal experiments than the 2D models, better predicting *in vivo* drug responses. Pickl *et al.* (44) observed that human breast cancer cell line SKBR-3 formed spheroids under three-dimensional culture conditions that were more sensitive to trastuzumab treatment than cells under 2D culture conditions. Further studies revealed that in 2D cultures, human epidermal growth factor receptor-2 (HER2) and human epidermal growth factor receptor-3 (HER3) formed heterodimers, whereas in multicellular spheroids, HER2 formed homodimers. Trastuzumab is a monoclonal antibody that specifically targets HER2. Therefore, in tumor spheroids, HER2 homodimerization leads to enhanced activation of HER2, thereby enhancing the inhibitory effect of trastuzumab on cancer cell proliferation. Additionally, a study has found that in the culture of non-small cell lung cancer cell lines HCC827 and HCC4006, EGFR phosphorylation is significantly upregulated in 3D cultures compared to 2D cell cultures (45). Therefore, it is speculated that the higher drug sensitivity observed under 3D culture conditions maybe because cells in 3D cultures better simulate the *in vivo* EGFR signaling of tumors.

In the future, we intend to examine more factors, such as other types of drugs and drug combinations. To develop a precise personalized medication regimen, we will further compare the sensitivities of anti-cancer drugs to the effects of clinical combination drugs. Notably, the TME is associated with patient prognosis and the treatment response because it can affect cancer multiplication, migration, and invasion (46). The 3D cell-laden model can mimic the *in vivo* growth conditions of lung cancer by vascularization (47), and multicellular co-cultures (48) with high efficiency.

Conclusions

In this study, we evaluated the feasibility of using SA and gelatin as hydrogel materials for the fabrication of 3D models and for applications in drug sensitivity testing. It has been shown that SA and gelatin are able to promote cell aggregation and better mimic the *in vivo* microenvironment. Compared with the 2D culture, the cells cultured in the 3D model showed higher levels of tumor stem cell marker expression, demonstrating that the 3D culture model can enhance the stemness properties of cancer cells. Further, the cells grown in the 3D culture were also less sensitive to drugs than those grown in the 2D culture. Culturing CRLCs directly from surgical specimens will facilitate screening assays to identify the most effective approach to treatment using conventional therapies, and thus provide insights into the development of novel individualized therapeutic regimes for lung cancer patients.

Acknowledgments

Funding: This work was supported by the Natural Science Foundation of Guangdong Province (Nos. 2023A1515030091 to Z.G., 2020B1515120094 to Y.D., and

2021B1515120053 to Y.T.).

Footnote

Reporting Checklist: The authors have completed the MDAR reporting checklist. Available at https://tlcr.amegroups.com/article/view/10.21037/tlcr-24-490/rc

Data Sharing Statement: Available at https://tlcr.amegroups.com/article/view/10.21037/tlcr-24-490/dss

Peer Review File: Available at https://tlcr.amegroups.com/article/view/10.21037/tlcr-24-490/prf

Conflicts of Interest: All authors have completed the ICMJE uniform disclosure form (available at https://tlcr.amegroups.com/article/view/10.21037/tlcr-24-490/coif). Z.G. reports funding support from the Natural Science Foundation of Guangdong Province (No. 2023A1515030091). Y.D. reports funding support from the Natural Science Foundation of Guangdong Province (No. 2020B1515120094). Y.T. reports funding support from the Natural Science Foundation of Guangdong Province (No. 2021B1515120053). The other authors have no conflicts of interest to declare.

Ethical Statement: The authors are accountable for all aspects of the work in ensuring that questions related to the accuracy or integrity of any part of the work are appropriately investigated and resolved. The study was conducted in accordance with the Declaration of Helsinki (as revised in 2013). The study was approved by the Ethics Committee of the First Affiliated Hospital, Sun Yat-sen University (No. [2018]-153) and informed consent was taken from all the patients.

References

1. Sung H, Ferlay J, Siegel RL, et al. Global Cancer Statistics 2020: GLOBOCAN Estimates of Incidence and Mortality Worldwide for 36 Cancers in 185 Countries. CA Cancer J Clin 2021;71:209-49.
2. Leiter A, Veluswamy RR, Wisnivesky JP. The global burden of lung cancer: current status and future trends. Nat Rev Clin Oncol 2023;20:624-39.
3. Duma N, Santana-Davila R, Molina JR. Non-Small Cell Lung Cancer: Epidemiology, Screening, Diagnosis, and Treatment. Mayo Clin Proc 2019;94:1623-40.
4. Vasan N, Baselga J, Hyman DM. A view on drug resistance in cancer. Nature 2019;575:299-309.
5. Liu X, Ory V, Chapman S, et al. ROCK inhibitor and feeder cells induce the conditional reprogramming of epithelial cells. Am J Pathol 2012;180:599-607.
6. Liu X, Krawczyk E, Suprynowicz FA, et al. Conditional reprogramming and long-term expansion of normal and tumor cells from human biospecimens. Nat Protoc 2017;12:439-51.
7. Yoshida GJ. Applications of patient-derived tumor xenograft models and tumor organoids. J Hematol Oncol 2020;13:4.
8. Palechor-Ceron N, Krawczyk E, Dakic A, et al. Conditional Reprogramming for Patient-Derived Cancer Models and Next-Generation Living Biobanks. Cells 2019;8:1327.
9. Tang Y, Lei Y, Huang S, et al. Pristimerin Exacerbates Cellular Injury in Conditionally Reprogrammed Patient-Derived Lung Adenocarcinoma Cells by Aggravating Mitochondrial Impairment and Endoplasmic Reticulum Stress through EphB4/CDC42/N-WASP Signaling. Oxid Med Cell Longev 2020;2020:7409853.
10. Arya AD, Hallur PM, Karkisaval AG,et al. Gelatin Methacrylate Hydrogels as Biomimetic Three-Dimensional Matrixes for Modeling Breast Cancer Invasion and Chemoresponse in Vitro. Acs Applied Materials & Interfaces 2016;8:22005.
11. Kim J, Koo BK, Knoblich JA. Human organoids: model systems for human biology and medicine. Nat Rev Mol Cell Biol 2020;21:571-84.
12. Bleijs M, van de Wetering M, Clevers H, et al. Xenograft and organoid model systems in cancer research. EMBO J 2019;38:e101654.
13. Biju TS, Priya VV, Francis AP. Role of three-dimensional cell culture in therapeutics and diagnostics: an updated review. Drug Deliv Transl Res 2023;13:2239-53.
14. Marchini A, Gelain F. Synthetic scaffolds for 3D cell cultures and organoids: applications in regenerative medicine. Crit Rev Biotechnol 2022;42:468-86.

15. Manduca N, Maccafeo E, De Maria R, et al. 3D cancer models: One step closer to in vitro human studies. Front Immunol 2023;14:1175503.
16. Liu Y, Zhou Y, Chen P. Lung cancer organoids: models for preclinical research and precision medicine. Front Oncol 2023;13:1293441.
17. López de Andrés J, Ruiz-Toranzo M, Antich C, et al. Biofabrication of a tri-layered 3D-bioprinted CSC-based malignant melanoma model for personalized cancer treatment. Biofabrication 2023.
18. He X, Jiang Y, Zhang L, et al. Patient-derived organoids as a platform for drug screening in metastatic colorectal cancer. Front Bioeng Biotechnol 2023;11:1190637.
19. Thilakan AT, Nandakumar N, Balakrishnan AR, et al. Development and characterisation of suitably bioengineered microfibrillar matrix-based 3D prostate cancer model forin vitrodrug testing. Biomed Mater 2023. doi:10.1088/1748-605X/acfc8e.
20. Świerczewska M, Sterzyńska K, Ruciński M, et al. The response and resistance to drugs in ovarian cancer cell lines in 2D monolayers and 3D spheroids. Biomed Pharmacother 2023;165:115152.
21. Jaiswal C, Mandal BB. A 3D In Vitro Triculture Hybrid Model Recapitulating Tumor Stromal Interaction of Triple-Negative Breast Cancer as a High Throughput Anticancer Drug Screening Platform. Advanced Therapeutics 2024. Available online: https://doi.org/10.1002/adtp.202300450
22. Sun L, Wang X, He Y, et al. Polyurethane scaffold-based 3D lung cancer model recapitulates in vivo tumor biological behavior for nanoparticulate drug screening. Regen Biomater 2023;10:rbad091.
23. Li W, Zhou Z, Zhou X, et al. 3D Biomimetic Models to Reconstitute Tumor Microenvironment In Vitro: Spheroids, Organoids, and Tumor-on-a-Chip. Adv Healthc Mater 2023;12:e2202609.
24. Bhattacharya A, Alam K, Roy NS, et al. Exploring the interaction between extracellular matrix components in a 3D organoid disease model to replicate the pathophysiology of breast cancer. J Exp Clin Cancer Res 2023;42:343.
25. Sun H, Sun L, Ke X, et al. Prediction of Clinical Precision Chemotherapy by Patient-Derived 3D Bioprinting Models of Colorectal Cancer and Its Liver Metastases. Adv Sci (Weinh) 2024;11:e2304460.
26. Lee KY, Mooney DJ. Alginate: properties and biomedical applications. Prog Polym Sci 2012;37:106-26.
27. Li Z, Guo J, Guan FC, et al. Oxidized sodium alginate cross-linked calcium alginate/antarctic krill protein composite fiber for improving strength and water resistance. Colloids and Surfaces a-Physicochemical and Engineering Aspects 2023;656:130317.
28. Loozen LD, Wegman F, Öner FC, et al. Porous bioprinted constructs in BMP-2 non-viral gene therapy for bone tissue engineering. J Mater Chem B 2013;1:6619-26.
29. Alipal J, Pu'ad NASM, Lee TC, et al. A review of gelatin: Properties, sources, process, applications, and commercialisation. Materials Today-Proceedings 2021;42:240-50.
30. Jaipan P, Nguyen A, Narayan RJ. Gelatin-based hydrogels for biomedical applications. Mrs Communications 2017;7:416-26.
31. Dong H, Li Z, Bian S, et al. Culture of patient-derived multicellular clusters in suspended hydrogel capsules for pre-clinical personalized drug screening. Bioact Mater 2022;18:164-77.
32. Reya T, Morrison SJ, Clarke MF, et al. Stem cells, cancer, and cancer stem cells. Nature 2001;414:105-11.
33. Ben-Porath I, Thomson MW, Carey VJ, et al. An embryonic stem cell-like gene expression signature in poorly differentiated aggressive human tumors. Nat Genet 2008;40:499-507.
34. Liu WJ, Du Y, Wen R, et al. Drug resistance to targeted therapeutic strategies in non-small cell lung cancer. Pharmacol Ther 2020;206:107438.
35. Lim ZF, Ma PC. Emerging insights of tumor heterogeneity and drug resistance mechanisms in lung cancer targeted therapy. J Hematol Oncol 2019;12:134.
36. Santo VE, Rebelo SP, Estrada MF, et al. Drug screening in 3D in vitro tumor models: overcoming current pitfalls of efficacy read-outs. Biotechnol J 2017. doi:10.1002/biot.201600505
37. Breslin S, O'Driscoll L. Three-dimensional cell culture: the missing link in drug discovery. Drug Discov Today 2013;18:240-9.
38. Dong QQ, Su X, Li X, et al. In vitro construction of lung cancer organoids by 3D bioprinting for drug evaluation. Colloids and Surfaces a-Physicochemical and Engineering Aspects 2023;666:131288.
39. Xie F, Sun L, Pang Y, et al. Three-dimensional bio-printing of primary human hepatocellular carcinoma for personalized medicine. Biomaterials 2021;265:120416.
40. Kim SK, Kim YH, Park S, et al. Organoid engineering with microfluidics and biomaterials for liver, lung disease, and cancer modeling. Acta Biomater 2021;132:37-51.
41. Khan AQ, Travers JB, Kemp MG. Roles of UVA radiation

and DNA damage responses in melanoma pathogenesis. Environ Mol Mutagen 2018;59:438-60.
42. Li L, Chen Y, Wang Y, et al. Effects of concentration variation on the physical properties of alginate-based substrates and cell behavior in culture. Int J Biol Macromol 2019;128:184-95.
43. Xiao RR, Jin L, Xie N, et al. Establishment and large-scale validation of a three-dimensional tumor model on an array chip for anticancer drug evaluation. Front Pharmacol 2022;13:1032975.
44. Pickl M, Ries CH. Comparison of 3D and 2D tumor models reveals enhanced HER2 activation in 3D associated with an increased response to trastuzumab. Oncogene 2009;28:461-8.
45. Lee HK, Noh MH, Hong SW, et al. Erlotinib Activates Different Cell Death Pathways in EGFR-mutant Lung Cancer Cells Grown in 3D Versus 2D Culture Systems. Anticancer Res 2021;41:1261-9.
46. Zeng Z, Li J, Zhang J, et al. Immune and stromal scoring system associated with tumor microenvironment and prognosis: a gene-based multi-cancer analysis. J Transl Med 2021;19:330.
47. Shirure VS, Hughes CCW, George SC. Engineering Vascularized Organoid-on-a-Chip Models. Annu Rev Biomed Eng 2021;23:141-67.
48. Cherne MD, Sidar B, Sebrell TA, et al. A Synthetic Hydrogel, VitroGel® ORGANOID-3, Improves Immune Cell-Epithelial Interactions in a Tissue Chip Co-Culture Model of Human Gastric Organoids and Dendritic Cells. Front Pharmacol 2021;12:707891.

Cite this article as: Zhao Z, Feng X, Wu H, Chen S, Ma C, Guan Z, Lei L, Tang K, Chen X, Dong Y, Tang Y. Construction of a lung cancer 3D culture model based on alginate/gelatin micro-beads for drug evaluation. Transl Lung Cancer Res 2024;13(10):2698-2712. doi: 10.21037/tlcr-24-490

